

## Supplementary Materials for

### The regulatory B cell–mediated peripheral tolerance maintained by mast cell IL-5 suppresses oxazolone-induced contact hypersensitivity

Hyuk Soon Kim, Min Bum Lee, Dajeong Lee, Keun Young Min, Jimo Koo, Hyun Woo Kim, Young Hwan Park, Su Jeong Kim, Masashi Ikutani, Satoshi Takaki, Young Mi Kim, Wahn Soo Choi\*

\*Corresponding author. Email: wahnchoi@kku.ac.kr

Published 17 July 2019, *Sci. Adv.* **5**, eaav8152 (2019)  
DOI: 10.1126/sciadv.aav8152

#### This PDF file includes:

- Fig. S1. Leukocyte population changes in mice with OXZ-induced CHS.
- Fig. S2. T<sub>reg</sub> cells are not essential for the development of IL-10<sup>+</sup> B<sub>reg</sub> cells in peripheral tissues.
- Fig. S3. The population changes in MCs, IL-13<sup>+</sup> ILC2s, and IL-10<sup>+</sup> B<sub>reg</sub> cells during OXZ-induced chronic atopic dermatitis (AD)–like skin inflammation.
- Fig. S4. Comparison of MCs and T<sub>reg</sub> cells in WT and *Cd19<sup>Cre</sup>* mice with CHS.
- Fig. S5. The treatment of IL-13 mAb suppresses OXZ-induced CHS in mice.
- Fig. S6. Analysis of B cells, T<sub>reg</sub> cells, and serum antibody isotypes from WT or *Kit<sup>W-sh/W-sh</sup>* mice.
- Fig. S7. CD40L on MCs is not critical for the suppression of CHS.
- Fig. S8. Amounts of T<sub>H1</sub> and T<sub>H2</sub> cytokines in peripheral tissues from WT or *Kit<sup>W-sh/W-sh</sup>* mice.
- Fig. S9. The tissue distribution of MCs in *Kit<sup>W-sh/W-sh</sup>* mice and B<sub>reg</sub> cells in *Cd19<sup>Cre</sup>* mice after the adoptive transfer of each cell.
- Fig. S10. The sorting strategies for B cell subsets, IL-13<sup>+</sup> ILC2s, and IL-10<sup>+</sup> B cells.

## SUPPLEMENTAL MATERIALS

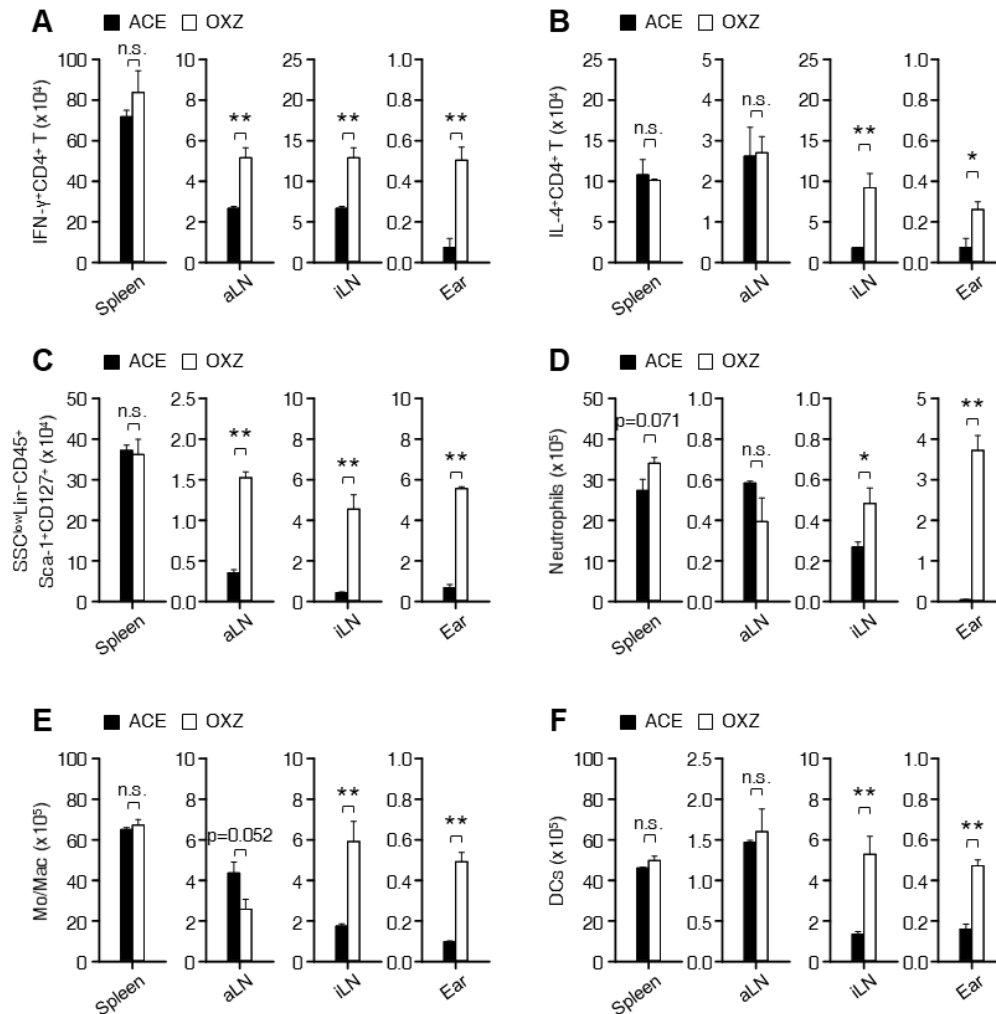


**Fig. S1. Leukocyte population changes in mice with OXZ-induced CHS.**

Analysis of primary leukocytes in spleen, aLN, iLN, and ear tissue from mice with or without OXZ treatment for 2 days. Histograms show the numbers of IFN- $\gamma$ <sup>+</sup>CD4<sup>+</sup> T cells (**A**), IL-4<sup>+</sup>CD4<sup>+</sup> T cells (**B**), total innate lymphoid cells (ILCs, Lin<sup>-</sup>CD45<sup>+</sup>CD127<sup>+</sup>Sca-1<sup>+</sup>) (**C**), neutrophils (CD11b<sup>+</sup>Gr-1<sup>+</sup>) (**D**), monocytes/macrophages (Mo/Mac, CD11b<sup>+</sup>F4/80<sup>±</sup>) (**E**), and dendritic cells (DCs, Gr-1<sup>-</sup>CD11c<sup>+</sup>) (**F**). All data are expressed as the mean  $\pm$  SEM from two independent experiments (n = 4 for each experiment). \**p* < 0.05; \*\**p* < 0.01; n.s., not significant versus ACE-treated group by Student's *t*-test.

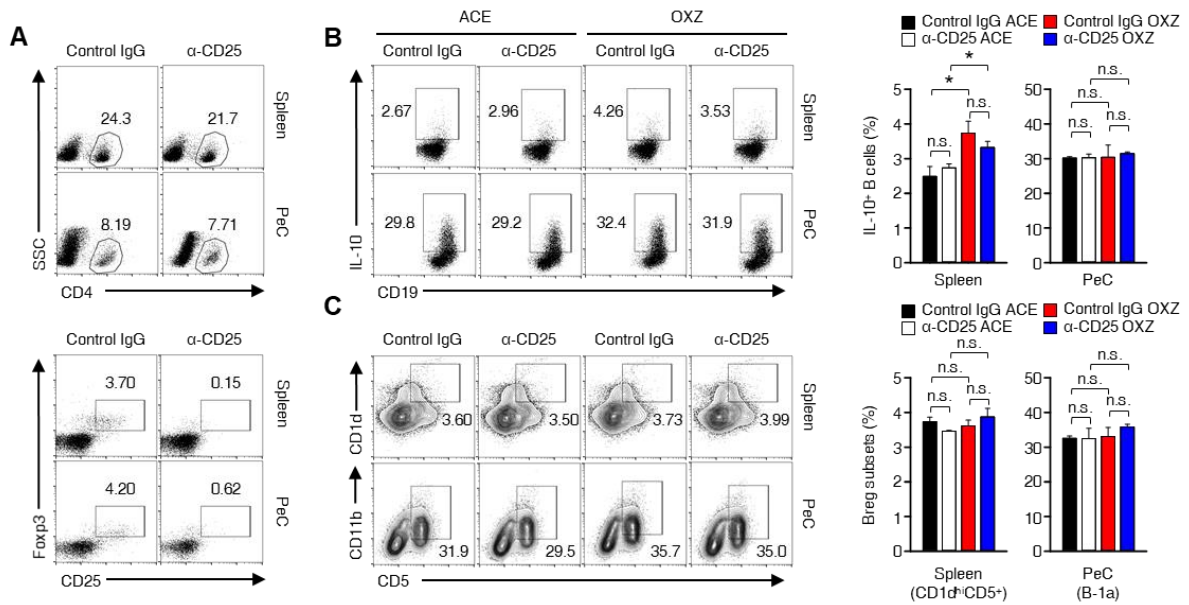


**Fig. S2. T<sub>reg</sub> cells are not essential for the development of IL-10<sup>+</sup> B<sub>reg</sub> cells in peripheral tissues.** (A to C) To deplete T<sub>reg</sub> cells, the mice were also injected i.p. with 250  $\mu$ g of an anti-CD25 mAb (PC61, Bio X Cell, West Lebanon, NH) twice on day -5 (sensitization) and day -1 (before challenge). The depletion of the cells was confirmed by flow cytometric analysis. (A) Representative flow cytometry images of CD4<sup>+</sup> T cells (upper) and Foxp3<sup>+</sup>CD25<sup>+</sup>CD4<sup>+</sup> T<sub>reg</sub> cells (lower) in the spleen and peritoneal cavity (PeC) are shown. Representative flow cytometry images (left) and frequencies (right) of IL-10<sup>+</sup> B cells (B) and CD1d<sup>hi</sup>CD5<sup>+</sup>CD19<sup>+</sup> B cells (e.g., CD5<sup>+</sup>CD11b<sup>+</sup>CD19<sup>+</sup> cells in the PeC) (C) are shown. All data are expressed as the mean  $\pm$  SEM from two independent experiments (n = 3 per group for each experiment). \**p* < 0.05; n.s., not significant by one-way ANOVA with post hoc Tukey's test.

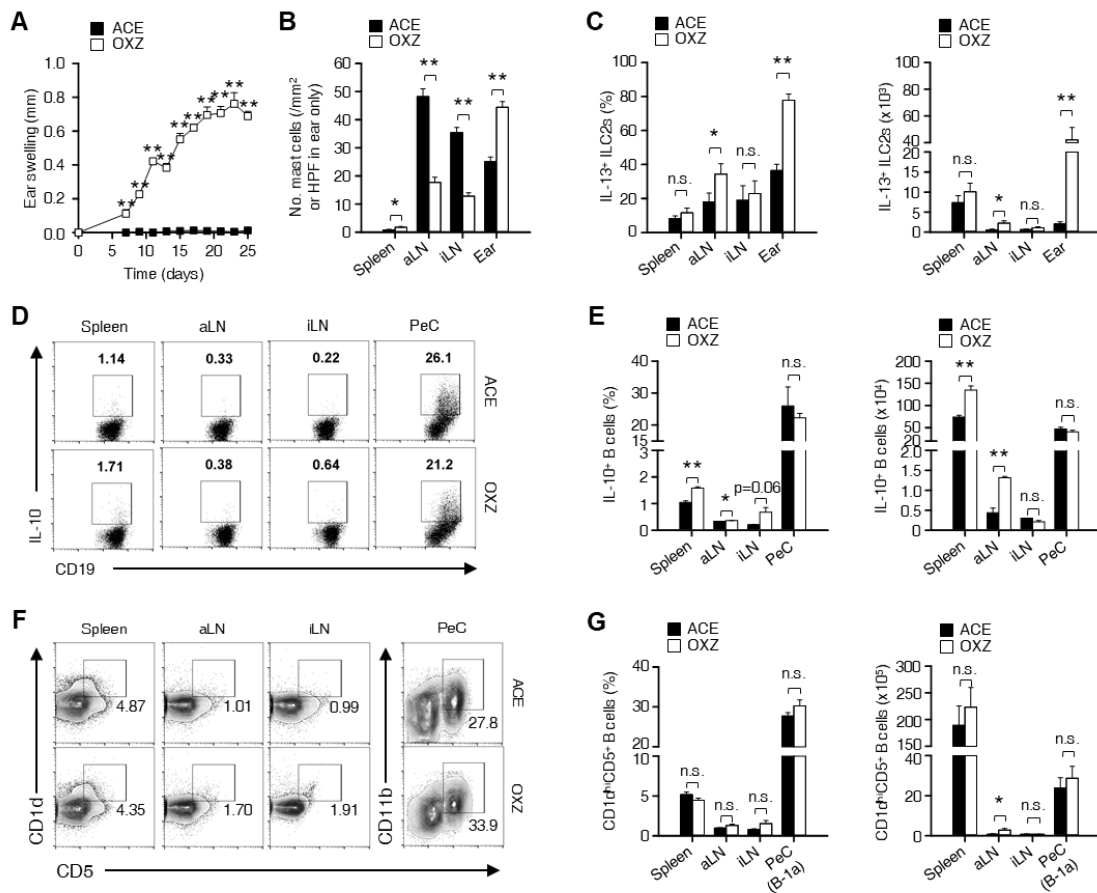


**Fig. S3. The population changes in MCs, IL-13<sup>+</sup> ILC2s, and IL-10<sup>+</sup> B<sub>reg</sub> cells during OXZ-induced chronic atopic dermatitis (AD)-like skin inflammation.** AD-like skin inflammation was induced by OXZ as previously reported (15). **(A)** The ear thickness of AD mice was measured for 25 days after sensitization with OXZ. **(B)** On day 25 after CHS induction by OXZ, the number of MCs by histology with toluidine blue. **(C to G)** Cells were analyzed by flow cytometer. **(C)** The frequency and number of IL-13<sup>+</sup>Lin<sup>-</sup>CD45<sup>+</sup>CD127<sup>+</sup>Sca-1<sup>+</sup> (IL-13<sup>+</sup> ILC2s) cells are shown. Representative images (D and F) and histograms (E and G) for IL-10<sup>+</sup> B cells, or CD1d<sup>hi</sup>CD5<sup>+</sup>CD19<sup>+</sup> cells (or CD5<sup>+</sup>CD11b<sup>+</sup>CD19<sup>+</sup> cells in the PeC) were presented as indicated. Data are expressed as the mean ± SEM (**A to C, E, and G**) or representative images (**D and F**) from three independent experiments (n ≥ 3 per group for each experiment). \*p < 0.05; \*\*p < 0.01; n.s., not significant by one-way ANOVA with post hoc Tukey's test.

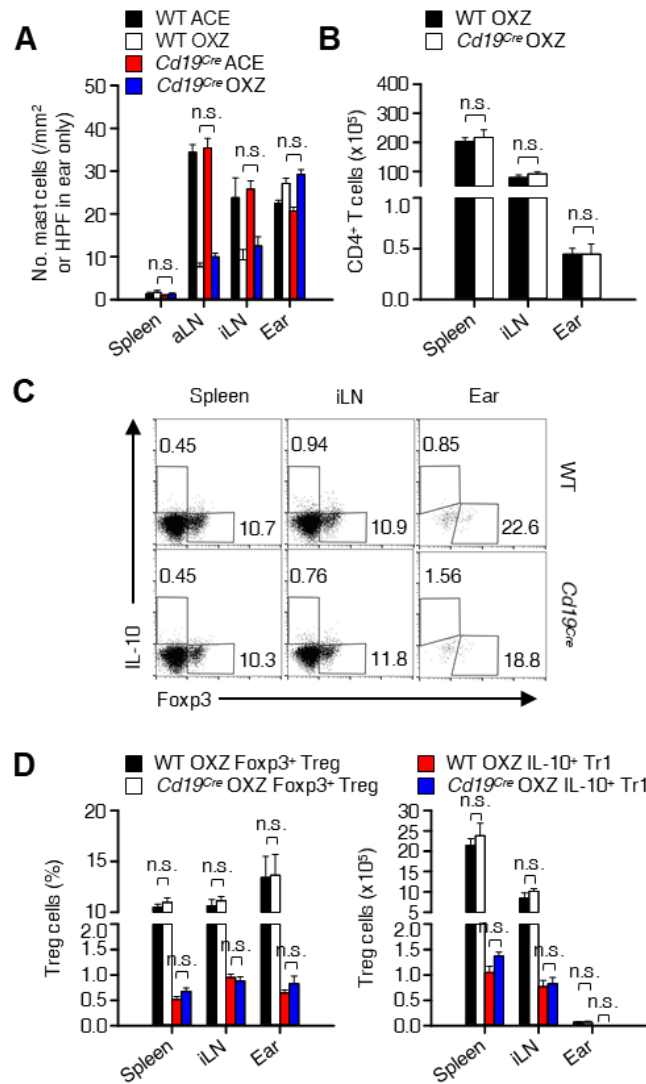


**Fig. S4. Comparison of MCs and T<sub>reg</sub> cells in WT and *Cd19<sup>Cre</sup>* mice with CHS. (A)**

The histograms show the number of MCs from histology images of ear tissues in WT or *Cd19<sup>Cre</sup>* mice. Results are shown as the mean  $\pm$  SEM from three independent experiments ( $n \geq 3$  per group for each experiment). (B) Number of CD4<sup>+</sup> T cells in spleen, iLN, and ear tissue from WT or *Cd19<sup>Cre</sup>* mice. Representative flow cytometry images (C) and the histograms for panel C (D) show the frequencies and numbers of IL-10<sup>+</sup> or Foxp3<sup>+</sup>CD4<sup>+</sup> T<sub>reg</sub> cells. (A, B, and D) Data are expressed as the mean  $\pm$  SEM from two independent experiments ( $n = 3$  per group for each experiment). n.s., not significant by Student's *t*-test.

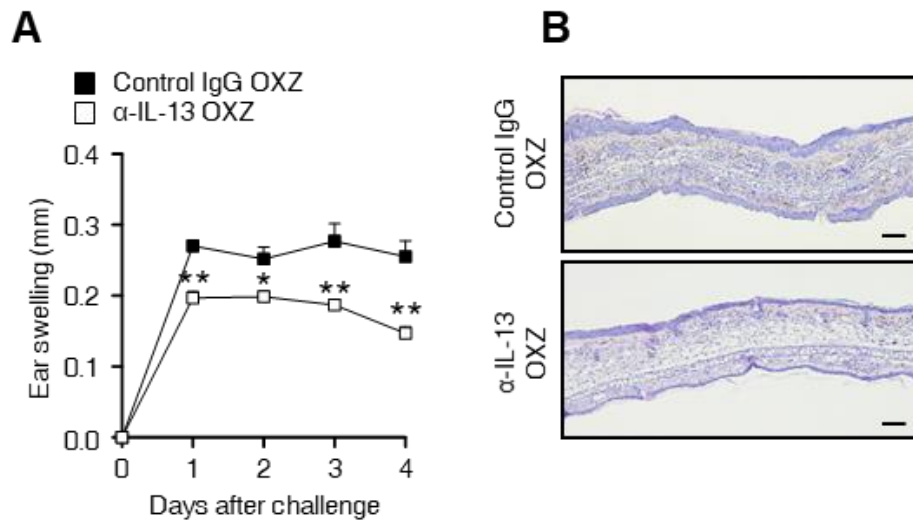


**Fig. S5. The treatment of IL-13 mAb suppresses OXZ-induced CHS in mice. (A)**

The mice were injected i.v. with 200  $\mu$ g of an anti-IL-13 mAb (8H8, Invivogen, San Diego, CA) or control IgG twice on day -1 (pre-challenge) and day 0 (1 hr before challenge). Ear thickness is measured for 4 days after challenge with OXZ. All

values are shown as the mean  $\pm$  SEM. **(B)** Four days after OXZ challenge, representative images of ear tissues stained with H&E are shown (scale bar, 100

$\mu$ m). **(A and B)** All data were obtained from two independent experiments ( $n = 3$  per group for each experiment). \* $p < 0.05$ ; \*\* $p < 0.01$  versus Control IgG by Student's  $t$ -test.

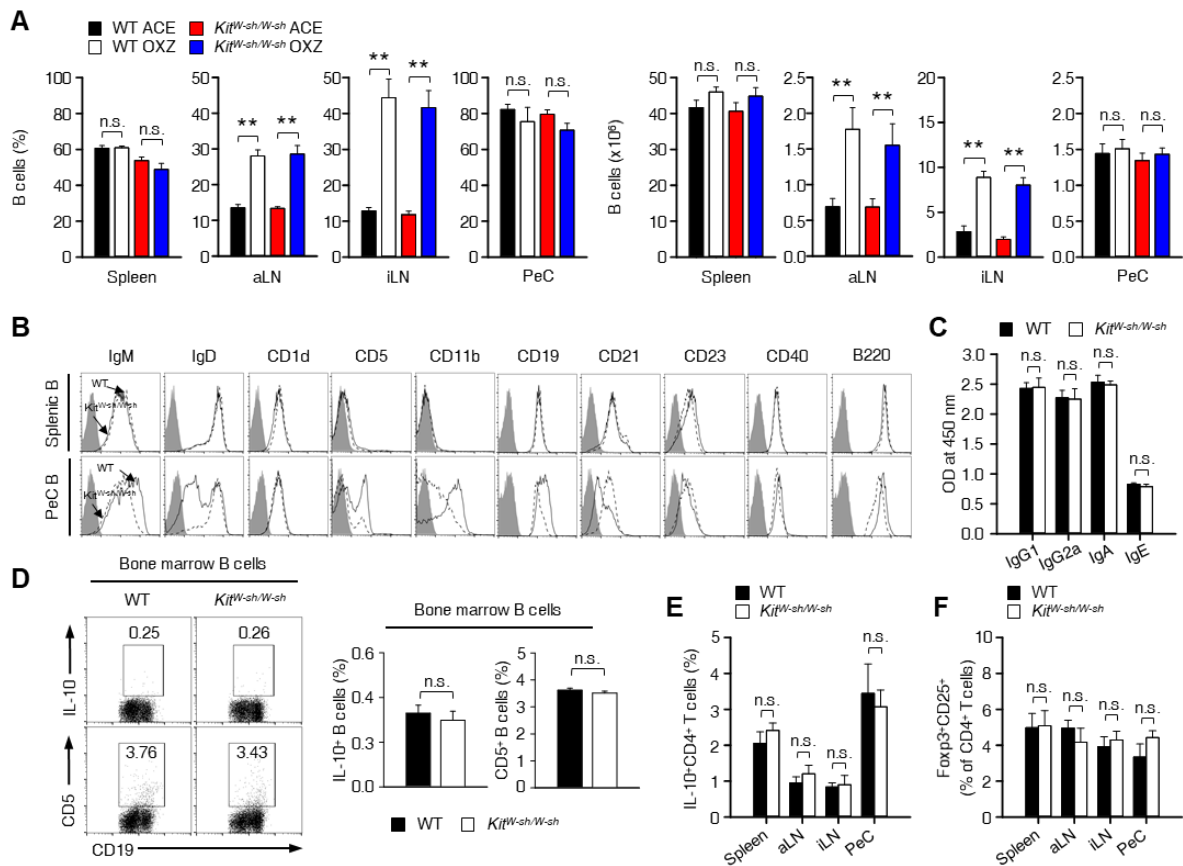


**Fig. S6. Analysis of B cells, T<sub>reg</sub> cells, and serum antibody isotypes from WT or *Kit<sup>W-sh/W-sh</sup>* mice.** (A) Frequencies (left) and numbers (right) of CD19<sup>+</sup> B cells in the spleen, aLN, iLN, and PeC with or without CHS were analyzed by flow cytometry. (B) Graphs for flow cytometric analysis of cell surface markers of splenic or PeC B cells are shown. (C) Serum concentrations of antibody isotypes. (D) Flow cytometry images (left) and frequencies (right) of IL-10<sup>+</sup> or CD5<sup>+</sup> bone marrow B cell subsets. (E) Frequency of IL-10<sup>+</sup>CD4<sup>+</sup> T cells and (F) Foxp3<sup>+</sup>CD25<sup>+</sup> (in CD4<sup>+</sup> T cells) are shown. The results are expressed as the mean ± SEM (A, C, D to F) or representative images (B and D) from two independent experiments (n = 3 per group for each experiment). \*\**p* < 0.01; n.s., not significant versus WT by Student's *t*-test.

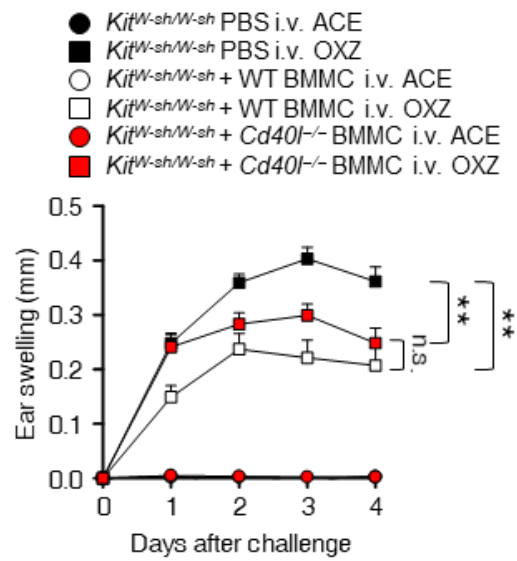


**Fig. S7. CD40L on MCs is not critical for the suppression of CHS.** Ear thickness of WT or *Kit*<sup>W-sh/W-sh</sup> mice with CHS induced by OXZ with or without the transfer of WT or *Cd40l*<sup>-/-</sup> BMMCs are measured. The data are expressed as the mean  $\pm$  SEM from two independent experiments ( $n \geq 4$  per group for each experiment). \*\* $p < 0.01$ ; n.s., not significant by one-way ANOVA with post hoc Tukey's test.



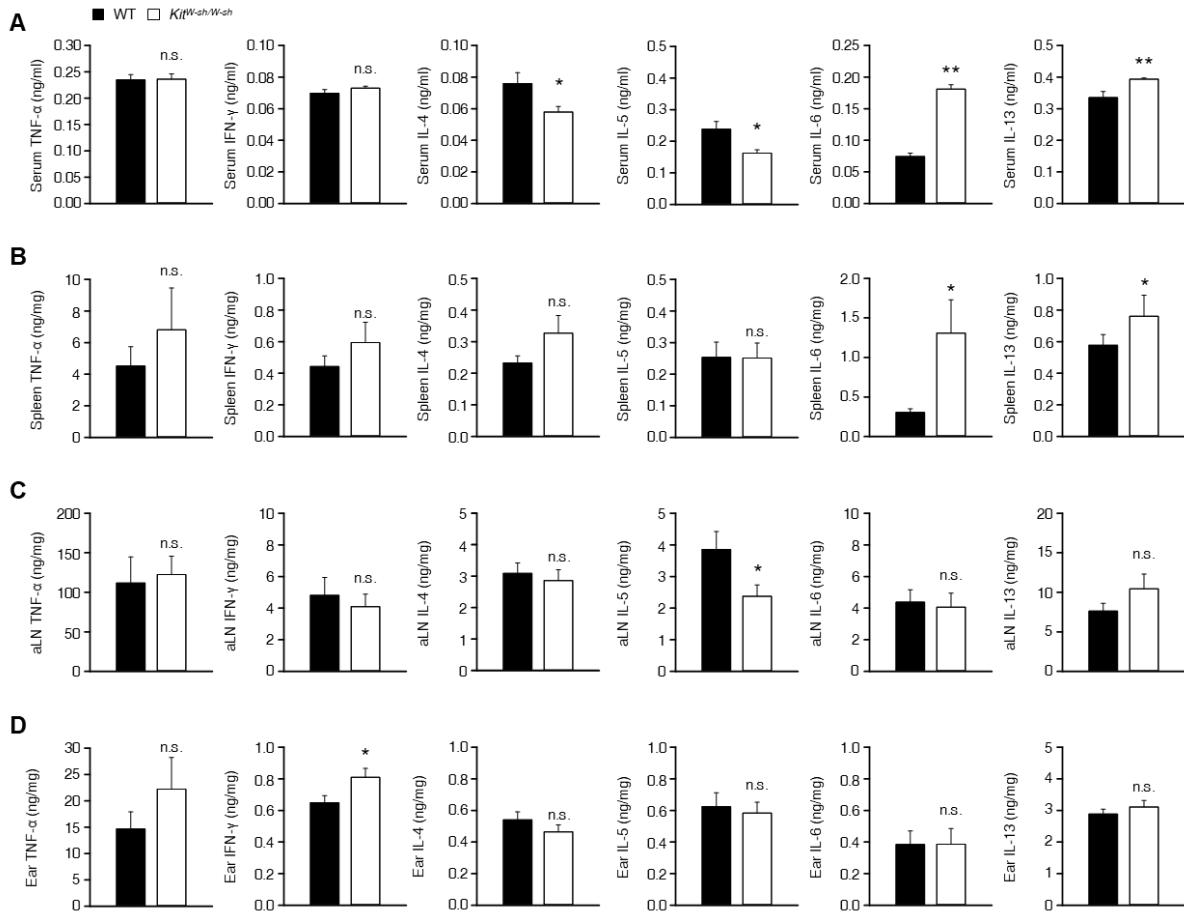


**Fig. S8. Amounts of T<sub>H</sub>1 and T<sub>H</sub>2 cytokines in peripheral tissues from WT or *Kit<sup>W-sh/W-sh</sup>* mice.** (A to D) The concentrations of T<sub>H</sub>1 and T<sub>H</sub>2 cytokines in the serum (A), spleen (B), aLN (C), and ear tissues (D) from WT or *Kit<sup>W-sh/W-sh</sup>* mice are measured by ELISA according to the manufacturers' instructions. All ELISA data are expressed as the mean ± SEM from at least two independent experiments (n ≥ 5 per group for each experiment). \*p < 0.05; \*\*p < 0.01; n.s., not significant versus WT by Student's *t*-test.

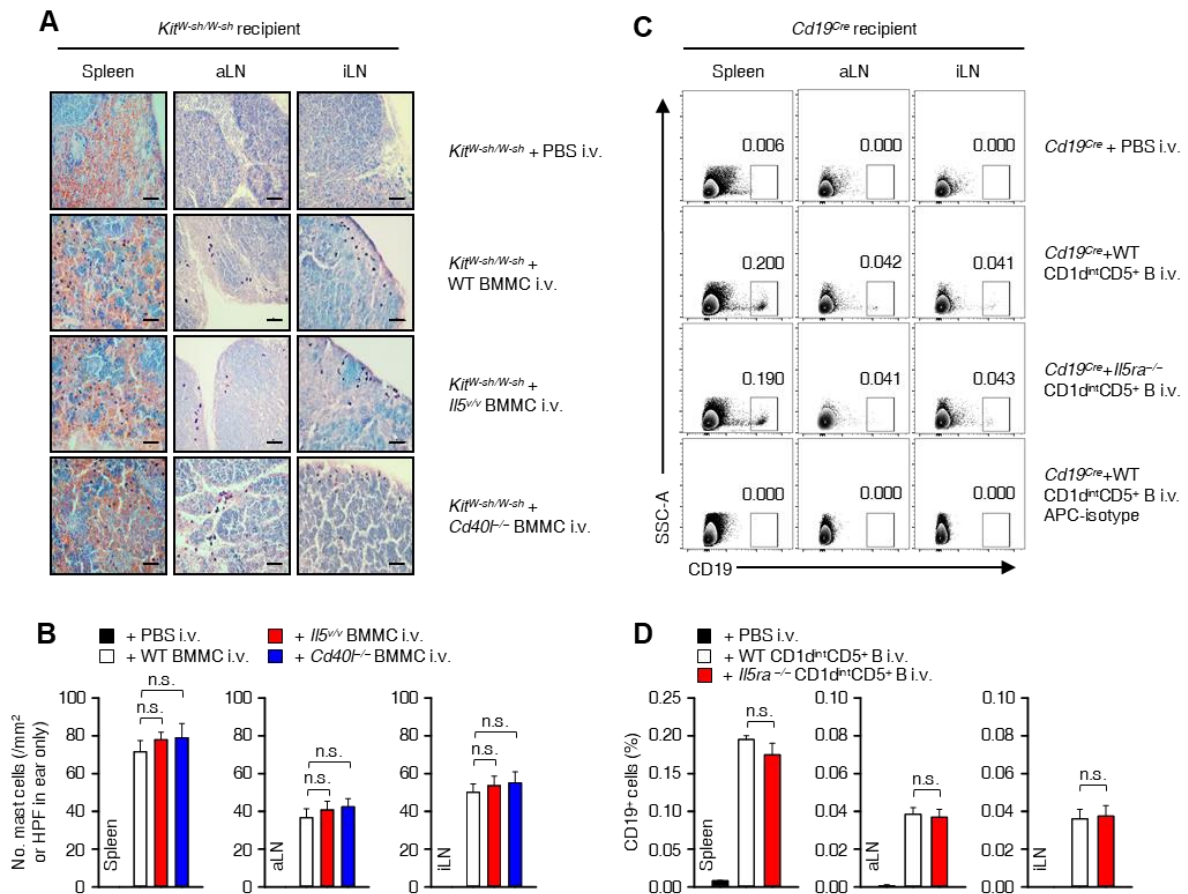


**Fig. S9. The tissue distribution of MCs in *Kit<sup>W-sh/W-sh</sup>* mice and B<sub>reg</sub> cells in *Cd19<sup>Cre</sup>* mice after the adoptive transfer of each cell. (A and B) WT, *I15<sup>+/+</sup>*, or *Cd40<sup>-/-</sup>* BMMCs ( $1 \times 10^7$  cells/mouse) were i.v. injected into recipient *Kit<sup>W-sh/W-sh</sup>* mice for 8 weeks. Representative images for MCs in spleen, aLN, and iLN (scale bar, 50  $\mu$ m) with toluidine blue are shown. (B) The histograms show the number of MCs for panel A. n.s., not significant versus WT BMMC i.v. transferred mice by Student's *t*-test. (C and D) For the adoptive transfer, each *CD1d<sup>int</sup>CD5<sup>+</sup>* B cell subset ( $1.5 \times 10^6$  cells/0.2 ml of PBS) was transferred i.v. into *Cd19<sup>Cre</sup>* mice. 4 days after injection, each Breg subset was analyzed by flow cytometry. (C) Representative images for spleen, aLN, and iLN are shown. (D) The histograms show the frequencies of *CD19<sup>+</sup>* adoptive transferred Breg cells for panel C. The results are expressed as the mean  $\pm$  SEM (A and C) or representative images (B and D) from two independent experiments ( $n = 3$  per group for each experiment). n.s., not significant by Student's *t*-test.**

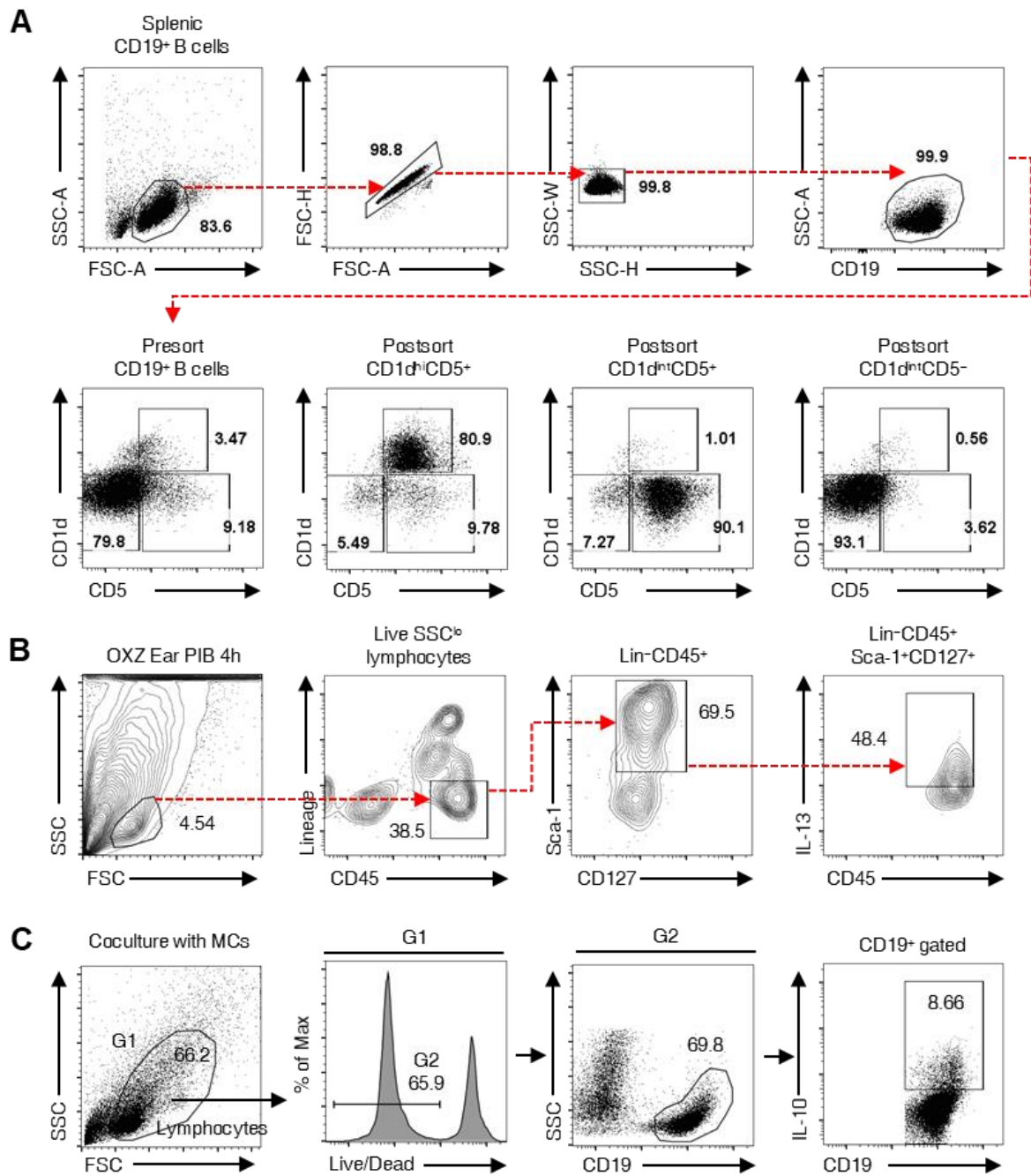


**Fig. S10. The sorting strategies for B cell subsets, IL-13<sup>+</sup> ILC2s, and IL-10<sup>+</sup> B cells.**

**(A)** Splenic CD1d<sup>hi</sup>CD5<sup>+</sup>, CD1d<sup>int</sup>CD5<sup>+</sup>, or CD1d<sup>int</sup>CD5<sup>-</sup> B cell subsets were isolated from mice by sorting with a FACSAria flow cytometer for adoptive transfer.

Representative flow cytometry images and purities of the sorted cells are shown. **(B)**

Single cells isolated from ear tissue were stimulated with phorbol 12-myristate 13-acetate (50 ng/ml), ionomycin (500 ng/ml), and brefeldin A (3 µg/ml) for 4 hr.

Lymphocytes were gated by SSC-A and FSC-A and then by FSC-A and FSC-H. Lin<sup>-</sup>

CD45<sup>+</sup> lymphocytes were further gated by CD127 and Sca-1. Analysis of IL-13<sup>+</sup> ILCs was performed with an anti-IL-13 antibody. Representative flow cytometry images

are shown. **(C)** Splenic CD19<sup>+</sup> B cells (1.5 × 10<sup>6</sup> cells/well) were cultured with or

without an equal number of BMDCs for 43 hr and with LPS (10 µg/ml), phorbol 12-myristate 13-acetate (50 ng/ml), ionomycin (500 ng/ml), and monensin (2 µM) for 5

hr, and the IL-10<sup>+</sup> B cells were analyzed by flow cytometry. After gating for

lymphocytes (G1), dead cells were excluded with the LIVE/DEAD Dye, and live B

cells were detected with an anti-CD19 monoclonal antibody (G2). Analysis of IL-10<sup>+</sup>

B cells was performed with an anti-IL-10 antibody. Representative images are shown.